Review of Gas Turbine Internal Cooling Improvement Technology

Article *in* Journal of Energy Resources Technology, Transactions of the ASME · August 2021

DOI: 10.1115/1.4048865

2 authors, including:

Farah Nazifa Nourin
University of Wisconsin–Milwaukee
26 PUBLICATIONS **269** CITATIONS

Review of Gas Turbine Internal Cooling Improvement Technology

Article *in* Journal of Energy Resources Technology · December 2020

DOI: 10.1115/1.4048865]

CITATIONS
0

READS
105

2 authors, including:

Farah Nazifa Nourin
University of Wisconsin - Milwaukee
13 PUBLICATIONS **25** CITATIONS

SEE PROFILE

Review of Gas Turbine Internal Cooling Improvement Technology

Farah Nazifa Nourin
Department of Mechanical Engineering,
University of Wisconsin-Milwaukee,
115 E. Reindl Way,
Glendale, WI 53212
e-mail: fnourin@uwm.edu

Ryoichi S. Amano[1]
Department of Mechanical Engineering,
University of Wisconsin-Milwaukee,
115 E. Reindl Way,
Glendale, WI 53212
e-mail: amano@uwm.edu

The higher firing temperature reflects the higher efficiency of the gas turbine. However, using higher temperatures is limited as it may cause a rupture, bending, or failure of the turbine blades. Hence, the development of an effective internal cooling system of the gas turbine blade is essential. At the same time, it is necessary to ensure the lowest possible penalty on the thermodynamics performance cycle. Researchers are working over the years to find out the efficient cooling channel design with high transfer while the lowest pressure drop. They ran several cases both numerically and experimentally. This paper reviews the published research in the various methods of gas turbine internal cooling, such as using rib turbulators, dimples, jet impingement, pin fins, and guide vane, of the gas turbine blade. [DOI: 10.1115/1.4048865]

Keywords: gas turbine blade, internal cooling, heat transfer, pressure drop, rib turbulators, dimples, jet impingement, pin fins, guide vanes, energy extraction of energy from its natural resource, energy systems analysis, heat energy generation/storage/transfer, power (co-) generation

Introduction

The gas turbine blade cooling can be divided into three major categories. They are (a) internal convective cooling, (b) film cooling, and (c) external cooling. Researchers are working continuously to improve the cooling technology to increase the gas turbine efficiency [1–8]. This study focuses on the internal cooling technologies that have been used during the last two decades. The internal convective cooling can be practiced using rib turbulators, pin fins, dimples, and jet impingement cooling (Fig. 1) [9]. Pin fin cooling is used in the trailing edge. An array of pins is arranged over the area, and when the air flows, the flow separates, and the horseshoe vortex is formed in the upstream direction. The dimple cooling method is used as an alternative to pin fin cooling as the pressure drop is relatively low. The rib turbulators are used in the middle portion of the airfoil. Jet impingement cooling is usually used near the leading edge region of the airfoil. The leading edge is suitable for this type of cooling, as this area is relatively thick. Air strikes the target surface. In these methods, the coolant passes through the region of interest and increases the heat transfer coefficient. The gas turbines have a wide range of applications. They are used in power generation, aircraft, tanks, ships, marine, etc. Different forms of internal cooling are reviewed in this study.

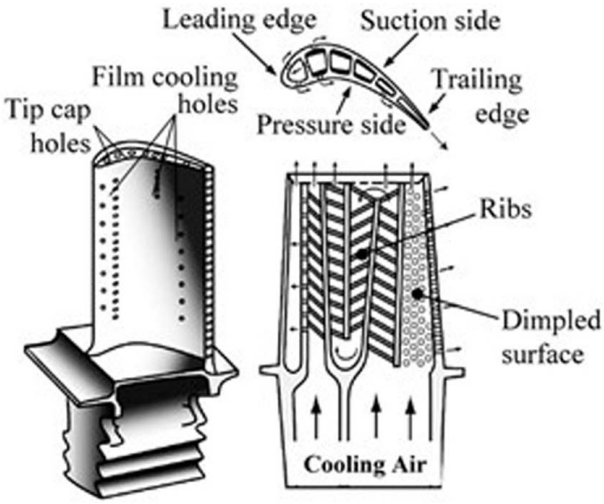

Fig. 1 Gas turbine internal cooling passage [9]

Rib Turbulators

In order to enhance the heat transfer in turbine blades, rib turbulators are mounted on the internal cooling passages. Ribs contribute to the flow separation at the top of the rib and again reattaches to the flow between the ribs—the turbulence of the flow increases due to the presence of ribs in the serpentine channels. Amano et al. [10] studied flow through a stationary ribbed channel for a gas turbine blade. They studied numerically using the Reynolds-stress model (RSM), k–ε, and k–ω for 45 deg and 90 deg angled ribbed and compared with the experimental results of Kyung et al. [11]. The characteristics of this numerical study are given in Table 1. They concluded that RSM and non-linear k–ω models are a right choice for the 90 deg angled rib as the RSM showed a good agreement with the experimental results of Nusselt number distribution and k–ω showed little deviation. Similarly, for 45 deg ribs, the simulation results show a better understanding of the RSM computations and agree with the experimental data. However, the k–ε and k–ω did not agree with the experimental results. The flow started to develop from the inlet leg. As a result, the upper portion of it

Table 1 Test section configurations [11]

Parameter	Unit (mm)
Hydraulic diameter (D_h)	40
Passage height (H)	40
Passage width (W)	40
Test section length (L)	552
Naphthalene coated length (ribbed channel)	214
Bleed hole diameter (d)	4.5
Rim thickness of hole	1
Hole-to-hole pitch (p_h)	22
Rib height (e)	2.2
Rib-to-rib pitch (p)	22

[1]Corresponding author.

Contributed by the Advanced Energy Systems Division of ASME for publication in the Journal of Energy Resources Technology. Manuscript received July 27, 2020; final manuscript received October 6, 2020; published online November 6, 2020. Editor: Hameed Metghalchi.

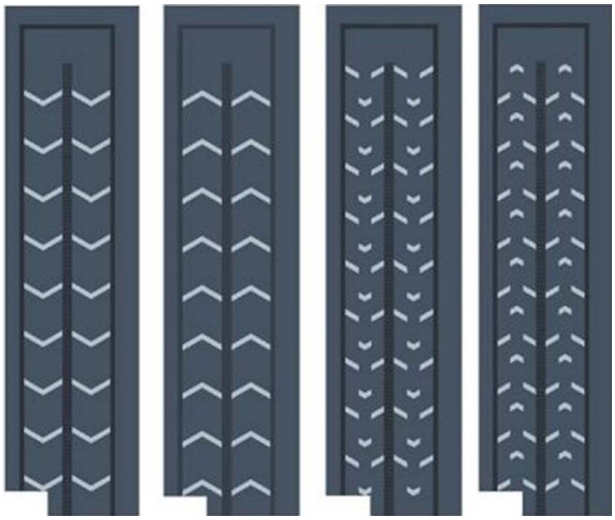

Fig. 2 Rib geometries of Hahn et al. [12]

Table 2 Average Nusselt number for each rib design [12]

Reynolds number 70,000		Reynolds number 90,000	
Rib design	Average Nusselt number	Rib design	Average Nusselt number
Plain	351.2	Plain	449.2
Geometry 1	517.1	Geometry 1	629.1
Geometry 2	520.2	Geometry 2	768.8
Geometry 3	602.0	Geometry 3	758.1
Geometry 4	718.2	Geometry 4	868.3

showed a slight decrease in heat transfer. Once the flow was fully developed, a recirculation zone is noticeable around the ribs and the bend section. The bend section revealed a significant increase in velocity. Hahn et al. [12] studied the heat transfer variations experimentally using different internal geometries. They focused on which rib geometry provides the highest heat transfer rate. They used a 0.0508×0.0508 m Plexiglas channel as an internal passage with Reynolds numbers 70,000 and 90,000. Four different rib geometries were tested. They are a 60 deg angle rib from its center, 60 deg angle rib from its center inversely positioned, 60 deg angle broken ribs, and 60 deg angle broken ribs inversely positioned in a staggered position (Fig. 2). Table 2 exemplifies that geometry 4 creates more heat transfer.

Chen et al. [13] introduced a guide vane with the ribbed wall in the serpentine channel shown in Fig. 3. According to this study, ribs within the turn have little influence on Nusselt number ratio distributions before and after the turn. The highest spatially averaged Nusselt number ratio distribution occurred in configuration (a). But the lowest overall pressure drop is found by configuration (b). Figure 4 shows the experimental results of normalized Nusselt number distribution for test Sec. 3 at $Re = 30{,}000$. Configurations (b) and (c) showed the same heat transfer distribution. They claimed that the ribs have little impact in the bend region to transfer the heat. Kamat et al. [14] investigated V-shaped ribs' effect on the internal cooling channel with 30 deg, 45 deg, and 60 deg angled ribs using ANSYS WORKBENCH. Three different aspect ratios were used in this study, and they were 1:1, 1:2, and 2:3. The V-shaped ribs were placed in the leading edge of the blade and pin-fins in the trailing edge as it is very thin and not suitable for the ribbed cooling. So, they used circular and triangular pin fins to increase the heat transfer rate in the trailing edge. The pin-fins increased the surface area and acted as turbulator, which resulted in overall heat transfer. The researchers concluded that ribs with 2:3 aspect

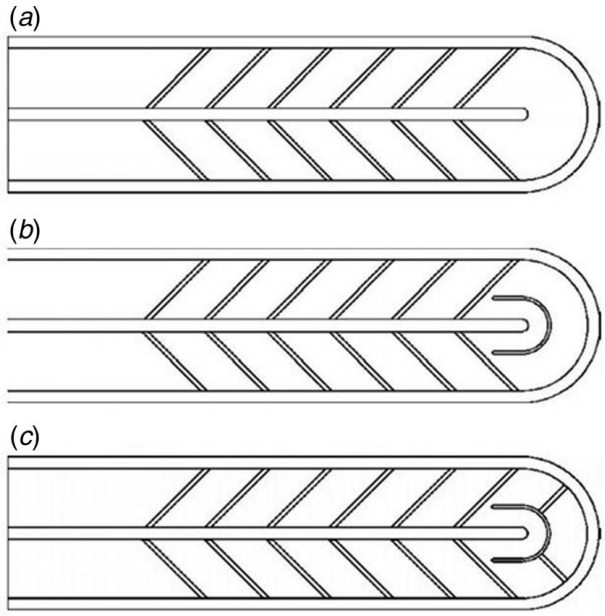

Fig. 3 Vane turning effect investigated by Chen et al. [13]: (*a*) Test section 1: without turning vane, (*b*) Test section 2: with turning vane, and (*c*) Test section 3: with turning vane and ribs in turn

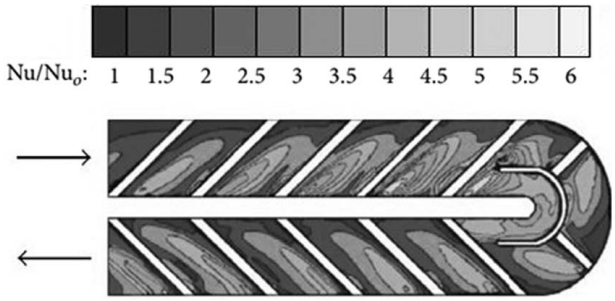

Fig. 4 Normalized Nusselt number distribution for test Sec. 3 at Re = 30,000 by Chen et al. [13]

ratios combined with a 45 deg rib and staggered triangular pin fins with 4-mm sides at the trailing edge represent the most effective heat transfer. This study claimed that using this configuration, and the blade temperature decreased by 47%.

Wang et al. [15] researched heat transfer phenomena in gas turbine blades with inclined ribs. After completing their experiment, they implemented it the rib roughness optimizing program for Rolls-Royce plc. The 60 deg inclined ribs produce a pair of counter-rotating vortices. The vortices lead the air from the center of the passage to the smooth wall adjacent to the leading edge of the ribs. The low cooling region was found at the core of the vortices. The research team described that the flow field behind parallel ribs was considerably affected by the secondary flows. They concluded that it might be because of the heat transfer coefficient contours do not run parallel to the ribs.

Another research team, Baggetta et al. [16] explored gas turbine blades internal cooling based on the 45 deg inclined rib turbulators. They studied three cases: (*a*) without intersecting rib, (*b*) with one intersecting rib, and (*c*) with two intersecting ribs (Fig. 5). Figure 5 illustrates a repetitive module of heat transfer distribution. The flow pattern is similarly described by Wang et al. [15]. Because of the influence of the secondary flows, the vortices move along the ribs and join with the mainstream. The moving vortices contain the core air at low temperatures, which affects the local heat transfer enhancement.

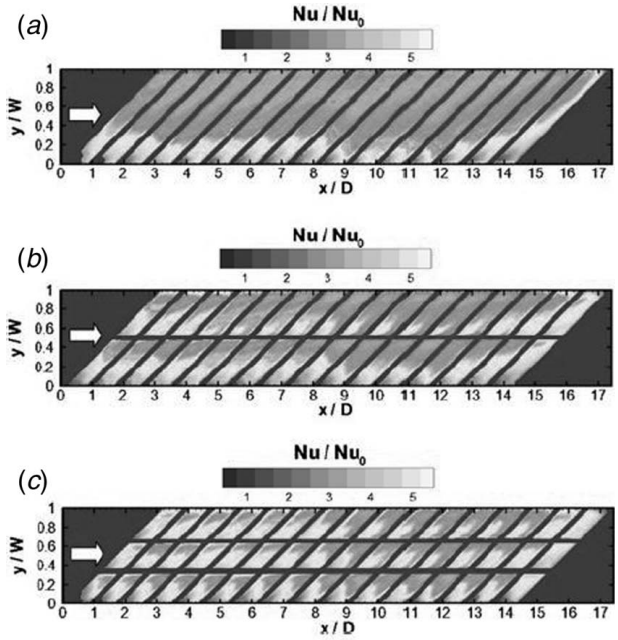

Fig. 5 Normalized Nusselt number ratio with 45 deg inclined rib at Re = 10,000: (*a*) without intersecting rib, (*b*) with one intersecting rib, and (c) with two intersecting ribs [16]

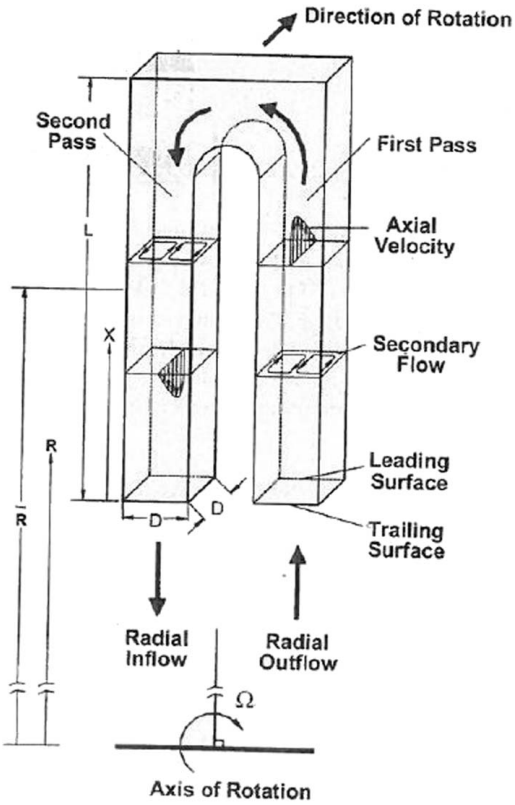

Fig. 6 Coolant flow through a two-pass rotating passage [18]

Wang et al. [17] investigated gas turbine internal flow characteristics with ribs, including film holes in the channel. To obtain a high heat transfer, they arranged the ribs asymmetrically of the suction side and put 40 film holes at the pressure side. The ribs were placed at a 60 deg-orientation. In this experimental study,

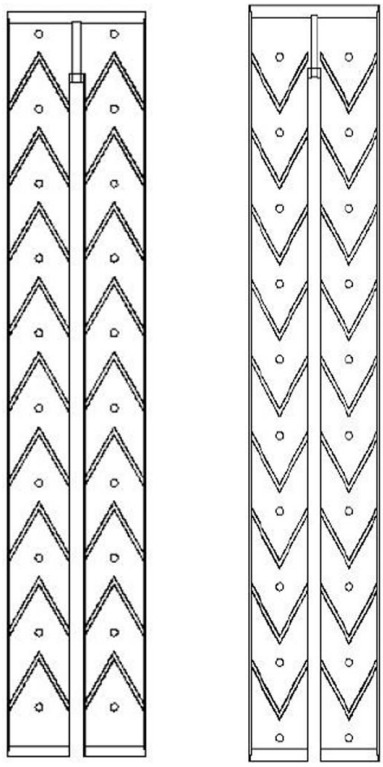

Fig. 7 V-ribs with bleed holes [19]

the research team established that in the upstream direction, if the bend in the first pass, the rib produces a symmetric pair of vortices. In the downstream direction, the air bubble was reduced by the rib. The ejection ratios (ratio between air comes from the main flow and auxiliary hole) from the trailing edge exits, and the film holes at the pressure side reduce the size of the secondary vortices downstream of the bend due to the variation of airflow. Han and Chen [18] discussed the effect of rotation in the rib turbulator channel (Fig. 6). Rotation in the channel stimulates centrifugal and Coriolis forces, which causes cross-stream secondary flow in the channel. That is why heat transfer phenomena are quite different in a rotating frame than a stationary frame. The result of their study shows that rotation increases heat transfer one side of the channel even though it reduces on the opposite side because of the secondary flow.

Kumar et al. [19] studied a two-pass channel with a V-rib and bleeding holes. The numerical study was conducted with Reynolds numbers 12,500 and 28,500 with 60 deg V-ribs. Figure 7 shows the rib and bleed holes arrangement. The inlet temperature was 593 K, and the cooling channel wall temperature was 300 K, considered as boundary conditions using k–ω SST model and RSM. This research reported that V-rib with bleed holes is suitable for heat transfer enhancement, and it delivers a steadiness between the mechanical and thermal design of a channel as bleed holes do not make the channel too heavy. The research team of Saravani et al. [20] reported on the effect of buoyancy and density ratio (i.e., cooling capacity) on a rotational smooth wall channel (see Fig. 8). The rotational speed was considered a maximum of 600 rpm, and the rotation number (which can be investigated using the centrifugal and Coriolis forces) considered was 0.75. The study concluded that with the increase of density ratio, the heat transfer ratio increased. The rotation introduces more buoyancy forces, which leads to a significant heat transfer enhancement. Another study of Saravani et al. [21] discussed a guide vane's effect in a parallel ribbed turbulated channel with rotation number 0.75. The study claims that including the guide vane increases the heat transfer after the turn region both for stationary and rotational cases.

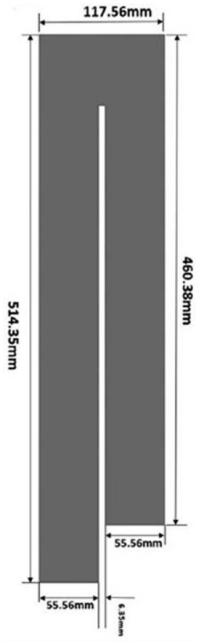

Fig. 8 Smooth wall channel used by Saravani et al. [20]

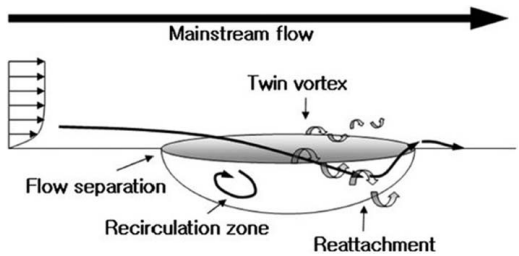

Fig. 9 Flow phenomena inside of the dimple [23]

Dimple Cooling

In the last few decades, dimples are got popular because of the low-pressure loss penalty compared with the rib turbulators or pin-fined channel. Mahmood et al. [22] studied local heat transfer and flow behavior of a cooling channel with a spherical dimpled surface. The experimental study was conducted Reynolds numbers ranging from 1250 to 61,500. The diameter and depth of the dimples are 50.80 mm and 10.2 mm, respectively. The flow visualization results show the vortex pair from the dimples. A vortex of fluid originates from the central region of a single dimple. Therefore, the enhancement of surface heat transfer happened, and a periodic production of an influx of fluid is found. Figure 9 shows the flow phenomena inside the dimple. Shin et al. [23] described that dimples separate the air stream's boundary layer using spherical dimples (the diameter and depth of the dimples are 16 mm and 4 mm, respectively) for Reynolds numbers varying from 30,000 to 50,000. A recirculation zone is created at the upstream side of the dimples. The separated flow again reattaches in the downstream side of the dimpled passage. The complex trends produce high and low heat transfer in and near the dimples.

Choi et al. [24] showed a combined study of the rib-dimpled channel. The channel aspect ratio is 4. The study was conducted with Reynolds numbers 30,000, 40,000, and 50,000. Figure 10 shows the geometry the researchers considered for the combined case. The rib thickness and height are 5 mm, and the rib pitch to the rib height ratio is 10. The dimple diameter is 11 mm, and a dimple depth to diameter ratio is 0.22. The three rows of dimples are aligned along the ribs. The results showed that the Nusselt number ratios and the thermal performance (ratio of heat transfer augmentation to the increase in pressure drop) for the rib-dimple cases were higher than the rib only cases. The alignment of the ribs and dimples increases the heat transfer augmentation as it gets more surface area. The study of Rao et al. [25] reported the heat transfer phenomena for four different types of dimples. The research team considered spherical, teardrop, elliptical, and inclined elliptical dimple (Fig. 11). Eleven rows of a staggered array of dimples inserted in the bottom surface of the passage with Reynolds numbers ranging from 8500 to 60,000. The diameter of the dimple was 20 mm, and the depth is 4 mm. The depth to diameter ratio was 0.2. Both the experimental and numerical results showed that the teardrop-dimpled channel improved heat transfer performance compared to the other dimpled channel while the pressure drop was higher in the case of the teardrop-dimpled channel.

Burgess and Ligrani [26] studied the effects of dimple depth on the internal cooling passage. Figure 12 shows the dimple geometries they considered in their study. There is three dimple depth to diameter (δ/D) ratios are considered, and they are 03, 0.2, and 0.1. The study concluded the deeper dimple depth resulted in higher heat transfer compared to the shallowest one. The study predicts that heat transfer increases with the increase of depth to diameter ratio as the deep dimples increase the vortices' strength and intensity. Nourin and Amano [27] reported dimple cooling with no bend two-pass channel and compared with the two-pass channel with the bend. The no bend dimpled channel shows better heat transfer as air creates both swirl flow and impingement on the heated surface.

Jet Impingement Cooling

Jet impingement cooling is highly efficient for the first stage vanes of the turbine blades. The cooling method is only used in the leading edge of the rotor blade as the structural constraints on the rotor blade under rotation, and centrifugal loads get highly heated. It is useful as the cooling air is delivered to impinge on the hot region. Jet impingement cooling performance depends on the geometry of the target plate, stand-off distance, arrangement of the nozzle holes, etc. Keenan et al. [28] conducted an experimental and numerical study on jet impingement cooling with single and double exit cases. They used 55 jet arrays with a constant heat flux condition. The stand-off distance was used $z/D = 3$, 4, and 5, with Reynolds numbers 8000, 12,000, and 15,000. The study reported that the peak value of the Nusselt number does not appear at the first jet on the plate. It appears at the second or the third nozzle for all cases. It is also worth mentioning that with the increase of standoff distance, the heat transfer rate decreases. The study of Amano et al. [29] also showed heat transfer behavior for the stand-off distance was used $z/D = 3$, 4, and 5. The study considered the V2F model, which is an advanced version of the standard k–ε model. They also considered k–ω, shear stress transport (SST), and k–ε model. The study represents the comparisons of different turbulence models with experimental results at single exit cases for Reynolds number = 15,000. The V2F model shows a more accurate prediction with the experimental results.

The effect of stand-off distance, i.e., the distance between the nozzle plate and target plate, was studied by Lee et al. [30]. The study was conducted for 1.5D, 3D, 5D, and 8D (D is the diameter of the nozzle) stand-off distance with Reynolds number ranging from 8000 to 50,000. They reported the same as Keenan et al. [28] that as the stand-off distance increases, the heat transfer rate decreases. Amano et al. [31] studied jet impingement with 1D, 2D, and 3D stand-off distance and also reported the highest heat transfer for the lowest stand-off distance. Another study of Amano et al. [32] researched on jet impingement with 3D, 5D, and 8D stand-off distances for inline and staggered nozzle array distribution. The staggered arrangement shows more distortion in jet trajectories. Pressure loss penalty is one of the drawbacks of the jet impingement cooling. Levy et al. [33] studied the pressure

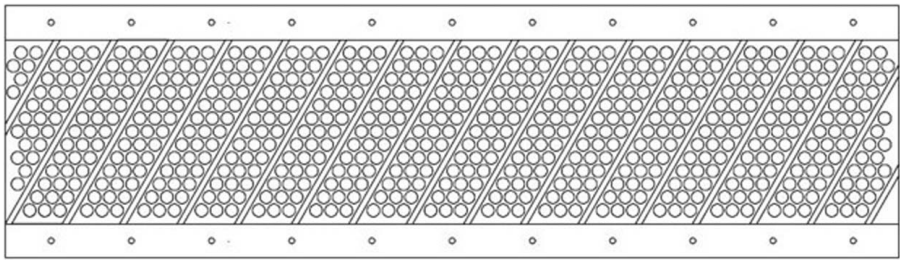

Fig. 10 Rib-dimpled case [24]

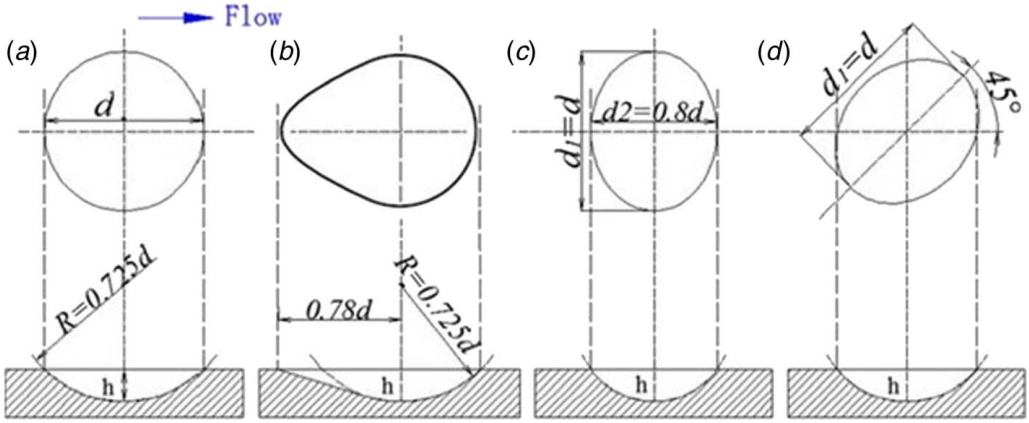

Fig. 11 Geometry of different types of dimples [25]: (*a*) spherical, (*b*) tear drop-shaped, (*c*) elliptical, and (*d*) inclined elliptical

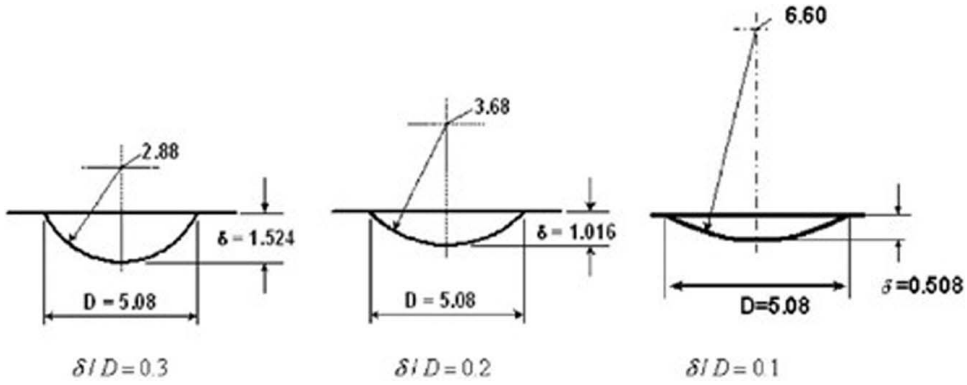

Fig. 12 Spherical dimples with different depth to diameter ratio [26]

loss effect for impingement cooling. Figure 13 represents the geometry considered for their study. The stand-off distance is 5D (here, nozzle diameter, $D = 0.4$ mm).

Figure 14 represents the pressure distribution along the channel. It is observed that pressure drop inside the channel is uniform. At the nozzle exit, non-uniformity appears because of crossflow. As the velocity of air rises, pressure increases from the channel to the air exit. Marzec and Kucaba-Pietal [34] reported the effect of different nozzle geometry on jet impingement cooling technology. Figure 15 shows four types of nozzle geometry. They are cylindrical short, cylindrical long, chamfer, and countersunk. The study was conducted with six nozzle jet arrays. The result shows that the chamfer nozzle has the largest deflection angle, whereas the countersunk nozzle has the lowest pressure drop. The highest pressure drop is found with the cylindrical nozzles due to the rapid increase

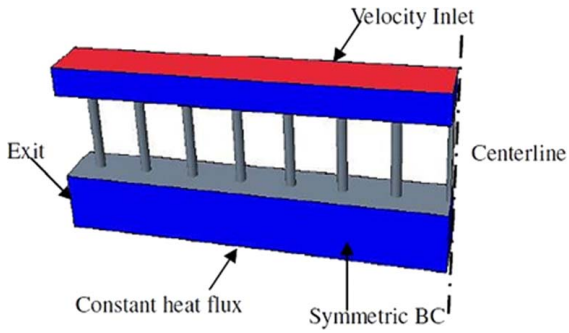

Fig. 13 Geometry of jet impingement arrangement with a single exit [33]

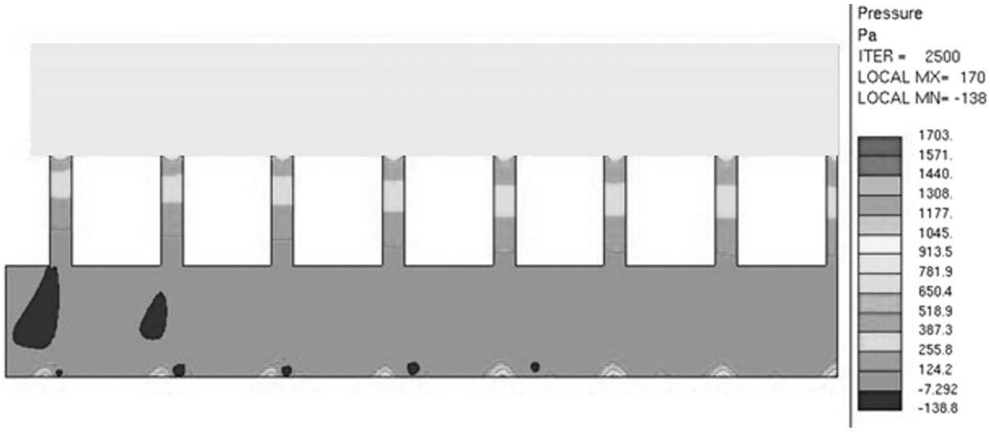

Fig. 14 Pressure distribution along the channel [33]

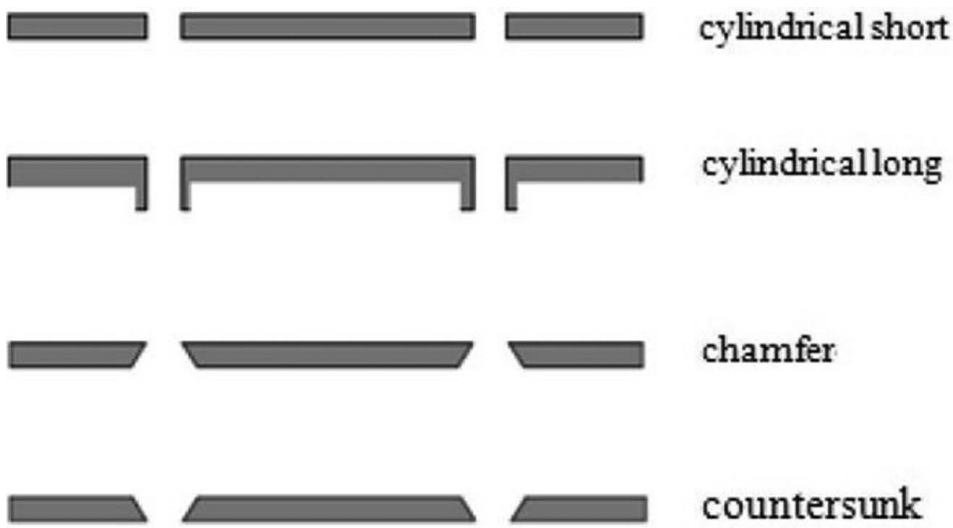

Fig. 15 Different nozzle geometry for jet impingement cooling [34]

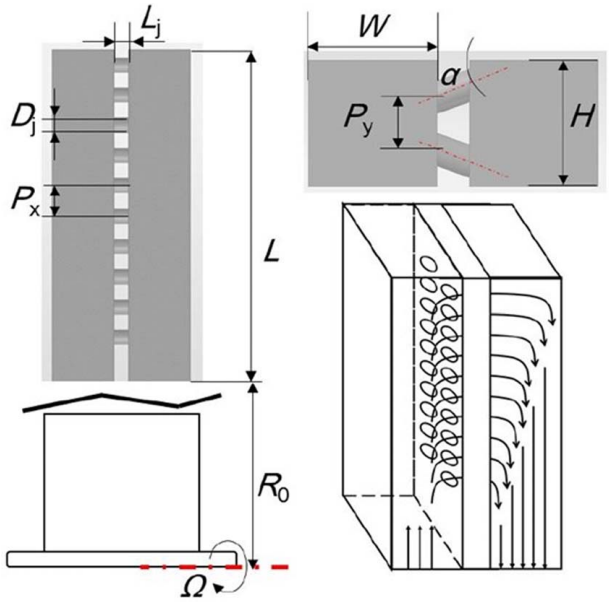

Fig. 16 Geometry of rotational jet impingement in a two-pass channel [35]

Table 3 Parameters used in the study of Yang et al. [35]

Parameter	Value
D_h (mm)	25.4
H/D	1
W/D	1
L/D	6
D_j (mm)	6.35
P_x/D	2
P_y/D	2
α (deg)	20
R_0/D	15.5
n	10
Ω	0, 250, 500, 750
Re	25,000, 50,000, 75,000, 100,000

of flowrate when entering the nozzle. The effect of rotation on jet impingement cooling in a two-channel was studied by Yang et al. [35]. Figure 16 and Table 3 shows the geometry and the parameters the research team used for their study. In the case of stationary case, the mass flowrate in jet holes decreases with the jet number with an exception for the last two jets. The last two jets show the exception due to the pressure change along with the upstream and downstream directions. In the upstream direction, continuous air withdrawal

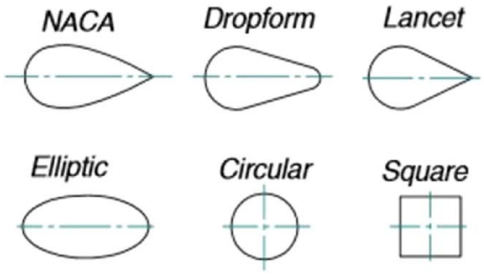

Fig. 17 Different shapes of pin-fins used by Sahiti et al. [37]

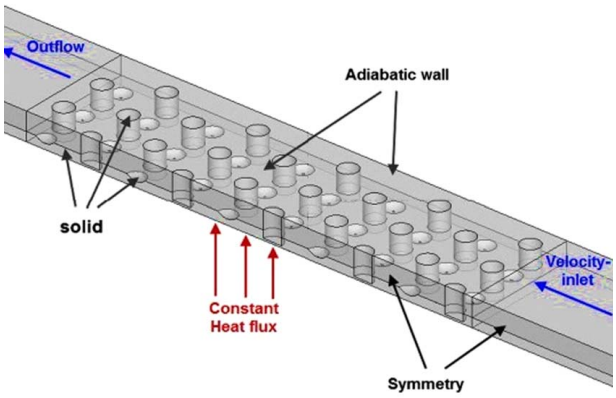

Fig. 18 Pin fin-dimpled channel [38]

reduces the flow speed and causes a static pressure rises from the inlet to the exit. In the downstream direction, the substantial pressure loss is found both by wall friction and by the mixing of jets and cross flow. In the rotational condition, the rotational number dominates because of the centrifugal force and pumping effect, the coolant transport to a higher radius. The Coriolis force causes an asymmetric flow distribution between the leading and trailing edge.

Pin Fin Cooling

Due to the limited space in the trailing edge of a gas turbine blade, pin-fins cooling is utilized in the trailing edge—the distribution of heat transfer is affected by the shape and geometry of the pin-fins. With the pin-fin arrangement, flow separation and wake drop at the downstream direction happens, and it causes the enhancement of the heat transfer. Brigham and VanFossen [36] studied the effect of pin-fins experimentally. They compared short and long pins and concluded that short pin-fins contribute to less heat transfer than the longer counterpart. Figure 17 shows the different shapes of pin-fins used by Sahiti et al. [37]. They studied on NACA, Drop form, Lancet, Elliptic, Circular, Square pin fins. They reported that the boundary layer separation occurs at different places of the pin-fins, depending on the shapes. The study concluded that the circular pin-fins show the best heat transfer performance even though the pressure drop is the highest, which comprises the efficiency of the channel.

Rao et al. [38] investigated the combined effect of pin fin-dimple array on the heat transfer enhancement and compared it with the pin-fin channel (Fig. 18). They considered the Reynolds number up to 54,000. The commercial solver FLUENT 6.3 was used for the computational study. The k–ε realizable model is used. According to the statement of the authors, the pin fin-dimpled channel shows better heat transfer enhancement and low-pressure drop than the pin-fin only channel for all Reynolds numbers as the dimples create more turbulence and vortices inside the channel.

A study by Shevchenko et al. [39] on the combination of pin fin-dimple reports similar results. Su et al. [40] studied the entropy generation of staggered pin fins. To reduce energy loss, it is essential to analyze the entropy generation. For small Reynolds number, entropy generation is dominated by thermal diffusion, but for large Reynolds number, it is dominated by fluid friction.

Conclusions

This review has discussed different types of internal cooling of gas turbine blades. It has summarized the research relevant to the gas turbine internal cooling. It has included both experimental and computational results, which was conducted by the researchers over the years. This review study has addressed heat transfer distribution briefly in attempt to simulate better technologies even though the better heat transfer depends on the materials and control systems. The summary will help the future researchers to focus on the critical issues to increase the efficiency of the gas turbine.

Different types of internal cooling methods correspond to that:

- The rib-turbulated cooling was used for a long time in the history of gas turbine cooling. It shows a better heat transfer enhancement than the smooth channel. But at the same time, the channel experiences a high-pressure drop, which reduces the channel efficiency.
- Because of the high-pressure drop with rib-turbulated cooling, engineers moved to dimple cooling and pin-fins cooling for trailing edge. The dimpled channel shows less pressure drop than the pin-finned passage. It represents a good agreement with the heat transfer augmentation and pressure drop.
- Jet impingement cooling is used in the leading edge of the turbine blade, where the rotor blade experiences the highest heat. Intense air-jet strikes at the wall region to transfer the heat.

Conflict of Interest

There are no conflicts of interest.

Nomenclature

D_h = hydraulic diameter, (mm)
R_0 = rotation number
Nu = Nusselt number
Re = Reynolds number

Greek Symbols

α = angle of jet
Ω = rotation speed

References

[1] Xie, G., Li, S., Zhang, W., and Sunden, B., 2013, "Computational Fluid Dynamics Modeling Flow Field and Side-Wall Heat Transfer in Rectangular Rib-Roughened Passages," ASME J. Energy Resour. Technol., **135**(4), p. 042001.
[2] Kamal, A., and Gollahalli, S. R., 2001, "Effects of Jet Reynolds Number on the Performance of Axisymmetric and Nonaxisymmetric Gas Burner Flames," ASME J. Energy Resour. Technol., **123**(2), pp. 167–172.
[3] Harvey, S. P., and Richter, H. J., 1994, "Gas Turbine Cycles With Solid Oxide Fuel Cells—Part II: A Detailed Study of a Gas Turbine Cycle With an Integrated Internal Reforming Solid Oxide Fuel Cell," ASME J. Energy Resour. Technol., **116**(4), pp. 312–318.
[4] Abdel Rahman, A., and Mokheimer, E., 2018, "Comparative Analysis of Different Inlet air Cooling Technologies, Including Solar Energy, to Boost Gas Turbine Combined Cycles in hot Regions," ASME J. Energy Resour. Technol., **140**(11), p. 112006.
[5] Khalil, A., Kayed, H., Hanafi, A., Nemitallah, M., and Habib, M., 2019, "Numerical Predictions of Three-Dimensional Unsteady Turbulent Film-Cooling for Trailing Edge of Gas-Turbine Blade Using Large Eddy Simulation," ASME J. Energy Resour. Technol., **141**(4), p. 042206.

[6] Forghan, F., Askari, O., Narusawa, U., and Metghalchi, H., 2016, "Cooling of Turbine Blade Surface With Expanded Exit Holes: Computational Suction-Side Analysis," ASME J. Energy Resour. Technol., **138**(5), p. 051602.
[7] Forghan, F., Askari, O., Narusawa, U., and Metghalchi, H., 2017, "Cooling of Turbine Blades With Expanded Exit Holes: Computational Analyses of Leading Edge and Pressure-Side of a Turbine Blade," ASME J. Energy Resour. Technol., **139**(4), p. 051602.
[8] Masci, R., and Sciubba, E., 2018, "A Lumped Thermodynamic Model of gas Turbine Blade Cooling: Prediction of First-Stage Blades Temperature and Cooling Flow Rates," ASME J. Energy Resour. Technol., **140**(2), p. 020901.
[9] Fransen, R., 2013, "LES Based Aerothermal Modeling of Turbine Blade Cooling Systems," Doctoral dissertation, Institute National Polytechnique de Toulouse—INPT.
[10] Amano, R. S., Guntur, K., Martinez Lucci, J., and Ashitaka, Y., 2010, "Study of Flow Through a Stationary Ribbed Channel for Blade Cooling," ASME Turbo Expo 2010: Power for Land, Sea, and Air, Glasgow, UK, June 14–18, pp. 471–478.
[11] Kim, K. M., Park, S. H., Jeon, Y. H., Lee, D. H., and Cho, H. H., 2007, "Heat/Mass Transfer Characteristics in Angled Ribbed Channels with Various Bleed Ratios and Rotation Numbers," ASME Turbo Expo 2007: Power for Land, Sea, and Air, Montreal, Canada, May 14–17, pp. 209–218.
[12] Hahn, T., Deakins, B., Buechler, A., Kumar, S., and Amano, R. S., 2012, "Experimental Analysis of the Heat Transfer Variations Within an Internal Passage of a Typical Gas Turbine Blade Using Varied Internal Geometries," ASME 2012 International Design Engineering Technical Conferences and Computers and Information in Engineering Conference, Chicago, IL, Aug. 12–15, pp. 851–858.
[13] Chen, W., Ren, J., and Jiang, H., 2011, "Effect of Turning Vane Configurations on Heat Transfer and Pressure Drop in a Ribbed Internal Cooling System," ASME J. Turbomach., **133**(4), p. 041012.
[14] Kamat, H., Shenoy, S. B., and Kini, C. R., 2017, "Effect of V-Shaped Ribs on Internal Cooling of Gas Turbine Blades," J. Eng. Technol. Sci., **49**(4), pp. 520–533.
[15] Wang, Z., Ireland, P. T., Kohler, S. T., and Chew, J. W., 1998, Heat Transfer Measurements to a Gas Turbine Cooling Passage With Inclined Ribs.
[16] Baggetta, L., Satta, F., and Tanda, G., 2019, "A Possible Strategy for the Performance Enhancement of Turbine Blade Internal Cooling With Inclined Ribs," Heat Transfer Eng., **40**(1–2), pp. 184–192.
[17] Wang, P., Pu, J., Yu, R. B., Wang, J. H., Wan, B., Luo, J. X., and Tian, S. Q., 2018, "An Experimental Investigation on Internal Flow Characteristics in a Realistic and Entire Coolant Channel with Ribs and Film Holes," ASME Turbo Expo 2018: Turbomachinery Technical Conference and Exposition, Oslo, Norway, June 11–15.
[18] Han, J. C., and Chen, H. C., 2006, "Turbine Blade Internal Cooling Passages With rib Turbulators," J. Propul. Power, **22**(2), pp. 226–248.
[19] Kumar, S., Amano, R. S., and Lucci, J. M., 2013, "Numerical Simulations of Heat Transfer Distribution of a two-Pass Square Channel With V-Rib Turbulator and Bleed Holes," Heat Mass Transfer, **49**(8), pp. 1141–1158.
[20] Saravani, M. S., DiPasquale, N. J., Beyhaghi, S., and Amano, R. S., 2019, "Heat Transfer in Internal Cooling Channels of Gas Turbine Blades: Buoyancy and Density Ratio Effects," ASME J. Energy Resour. Technol., **141**(11), p. 112001.
[21] Saravani, M. S., Amano, R. S., DiPasquale, N. J., and Halmo, J. W., 2020, "Turning Guide Vane Effect on Internal Cooling of Two-Passage Channel with Parallel Ribs," ASME J. Energy Resour. Technol., **142**(9), p. 091303.
[22] Mahmood, G. I., Hill, M. L., Nelson, D. L., Ligrani, P. M., Moon, H. K., and Glezer, B., 2001, "Local Heat Transfer and Flow Structure on and Above a Dimpled Surface in a Channel," ASME J. Turbomach., **123**(1), pp. 115–123.
[23] Shin, S., Lee, K. S., Park, S. D., and Kwak, J. S., 2009, "Measurement of the Heat Transfer Coefficient in the Dimpled Channel: Effects of Dimple Arrangement and Channel Height," J. Mech. Sci. Technol., **23**(3), pp. 624–630.
[24] Choi, E. Y., Choi, Y. D., and Kwak, J. S., 2013, "Effect of Dimple Configuration on Heat Transfer Coefficient in a Rib-Dimpled Channel," J. Thermophys. Heat Transfer, **27**(4), pp. 653–659.
[25] Rao, Y., Feng, Y., Li, B., and Weigand, B., 2015, "Experimental and Numerical Study of Heat Transfer and Flow Friction in Channels with Dimples of Different Shapes," ASME J. Heat Transfer, **137**(3), p. 031901.
[26] Burgess, N. K., and Ligrani, P. M., 2005, "Effects of Dimple Depth on Channel Nusselt Numbers and Friction Factors," ASME J. Heat Transfer, **127**(8), pp. 839–847.
[27] Nourin, F. N., and Amano, R. S., 2020, "Study on Heat Transfer Enhancement of Gas Turbine Blades," Int. J. Energy Clean Environ., **21**(2), pp. 91–106.
[28] Keenan, M., Amano, R. S., and Ou, S., 2013, "Study of an Impingement Cooling jet Array for Turbine Blade Cooling with Single and Double Exit Cases," ASME Turbo Expo 2013: Turbine Technical Conference and Exposition, San Antonio, TX, June 3–7.
[29] Amano, R. S., Keenan, M., and Ou, S., 2014, *Impingement Jet Cooling in Gas Turbines*, R. S. Amano, and B Sunden, eds., WIT Press, UK, pp. 33–62.
[30] Lee, J., Ren, Z., Ligrani, P., Fox, M. D., and Moon, H. K., 2015, "Crossflows From jet Array Impingement Cooling: Hole Spacing, Target Plate Distance, Reynolds Number Effects," Int. J. Therm. Sci., **88**, pp. 7–18.
[31] Amano, R. S., Nourin, F. N., Salem, A. R. S., and DiPasquale, N., 2019, "Investigation of Experimental Jet Array for Impinging Cooling of Blades," AIAA Propulsion and Energy 2019 Forum, Indianapolis, IN, Aug. 19–22, p. 4240.
[32] Salem, A., Nourin, F., Abousabae, M., and Amano, R.S., 2020, "Experimental and Numerical Study of Jet Impingement Cooling for Improved Gas Turbine Blade Internal Cooling with In-Line and Staggered Nozzle Arrays," ASME J. Energy Resour. Technol., **143**(1), p. 012103.
[33] Levy, Y., Rao, A. G., Erenburg, V., Sherbaum, V., Gaissinski, I., and Krapp, V., 2012, "Pressure Losses for Jet Array Impingement With Crossflow," ASME Turbo Expo 2012: Turbine Technical Conference and Exposition, Copenhagen, Denmark, June 11–15, pp. 139–149.
[34] Marzec, K., and Kucaba-Pietal, A., 2014, "Heat Transfer Characteristic of an Impingement Cooling System With Different Nozzle Geometry," Journal of Physics: Conference Series, Krakow, Poland, June 15–18, IOP Publishing, p. 012038.
[35] Yang, L., Tyagi, K., Ekkad, S., and Ren, J., 2015, "Influence of Rotation on Heat Transfer in a Two-Pass Channel With Impingement Under High Reynolds Number," ASME Turbo Expo 2015: Turbine Technical Conference and Exposition, Montreal, Quebec, Canada, June 15–19.
[36] Brigham, B. A., and VanFossen, G. J., 1984, "Length to Diameter Ratio and Row Number Effects in Short pin fin Heat Transfer," ASME J. Gas Turbines Power, **106**(1), pp. 241–245.
[37] Sahiti, N., Lemouedda, A., Stojkovic, D., Durst, F., and Franz, E., 2006, "Performance Comparison of pin fin in-Duct Flow Arrays With Various pin Cross-Sections," Appl. Therm. Eng., **26**(11–12), pp. 1176–1192.
[38] Rao, Y., Xu, Y., and Wan, C., 2012, "An Experimental and Numerical Study of Flow and Heat Transfer in Channels With Pin Fin-Dimple and pin fin Arrays," Exp. Therm. Fluid. Sci., **38**, pp. 237–247.
[39] Shevchenko, I., Kindra, V., and Bychkov, N., 2018, "A Numerical Study of Heat and Mass Transfer in a Narrowing Channel With Pin Fin-Dimple Arrays," 2018 International Multi-Conference on Industrial Engineering and Modern Technologies (FarEastCon), Vladivostok, Russia, Oct. 3–4, IEEE, pp. 1–4.
[40] Su, Y., Liu, Z., and Jiang, F., 2011, "Entropy Generation of Staggered Short pin fin Arrays," 2011 International Conference on Remote Sensing, Environment and Transportation Engineering, Nanjing, China, June 24–26, IEEE, pp. 300–303.